K^-/K^+ ratio in heavy-ion collisions with an antikaon self-energy in hot and dense matter

Laura Tolós, Artur Polls, and Angels Ramos

Departament d'Estructura i Constituents de la Matèria, Universitat de Barcelona, Diagonal 647, 08028 Barcelona, Spain

Jürgen Schaffner-Bielich

Institut für Theoretische Physik, J. W. Goethe-Universität, D-60054 Frankfurt am Main, Germany
(Received 21 February 2003; published 15 August 2003)

The K^-/K^+ ratio produced in heavy-ion collisions at GSI energies is studied. The in-medium properties at finite temperature of the hadrons involved are included, paying special attention to the in-medium properties of antikaons. Using a statistical approach, it is found that the determination of the temperature and chemical potential at freeze-out conditions compatible with the ratio K^-/K^+ is very delicate, and depends very strongly on the approximation adopted for the antikaon self-energy. The use of an energy-dependent $\bar{K}$ spectral density, including both s- and p-wave components of the $\bar{K}N$ interaction, lowers substantially the freeze-out temperature compared to the standard simplified mean-field treatment and gives rise to an overabundance of K^- production in the dense and hot medium. Even a moderately attractive antikaon-nucleus potential obtained from our self-consistent many-body calculation does reproduce the "broadband equilibration" advocated by Brown, Rho, and Song due to the additional strength of the spectral function of the K^- at low energies.

I. INTRODUCTION

The study of the properties of hadrons in hot and dense matter is receiving a lot of attention in recent years to understand fundamental aspects of the strong interaction, such as the partial restoration of chiral symmetry [1–3], as well as a variety of astrophysical phenomena, such as the dynamical evolution of supernovae and the composition of neutron stars [4].

A special effort has been invested to understand the properties of antikaons in the medium, especially after the speculation of the possible existence of an antikaon condensed phase was put forward in Ref. [5] which would soften the equation of state producing, among other phenomena, lower neutron star masses [6–8].

While it is well established that the antikaons should feel an attractive interaction when they are embedded in a nuclear environment, the size of this attraction has been the subject of intense debate. Theoretical models including medium effects on the antikaon-nucleon scattering amplitude, the behavior of which is governed by the isospin zero $\Lambda(1405)$ resonance, naturally explain the evolution from repulsion in free space to attraction in the nuclear medium [9,10]. However, the presence of the resonance makes the size of the antikaon-nucleus potential very sensitive to the many-body treatment of the medium effects. The phenomenological attempts of extracting information about the antikaon-nucleus potential from kaonic-atom data favored very strongly attractive well depths [11], but recent self-consistent in-medium calculations [12–15] based on chiral Lagrangian's [10,16] or meson-exchange potentials [17] predict a moderately attractive kaon-nucleus interaction. In fact, recent analyses of kaonic atoms [18–20] are able to find a reasonable reproduction of the data with relative shallow antikaon-nucleus potentials, therefore indicating that kaonic atom data cannot really pin down the strength of the antikaon-nucleus potential at nuclear matter saturation density.

On the other hand, heavy-ion collisions at energies around 1–2A GeV offer the possibility of studying experimentally the properties of a dense and hot nuclear system [21–23]. In particular, a considerable amount of information about strange particles such as antikaons is available. Since antikaons are produced at finite density and finite momentum, the chiral models have recently incorporated the higher partial waves of the antikaon-nucleon scattering amplitude both in free space [24–26] and in the nuclear medium [27,28]. The complete scenario taking into account finite density, finite momentum, and finite temperature has recently been addressed in Refs. [14,29].

Event generators trying to analyze heavy-ion collision data [30–36] need to implement the modified properties of the hadrons in the medium where they are produced. Transport models have shown, for instance, that the multiplicity distributions of kaons and antikaons are much better reproduced if in-medium masses rather than bare masses are used [37,38]. Production and propagation of kaons and antikaons have been investigated with the Kaon Spectrometer (KaoS) of the SIS heavy-ion synchrotron at GSI (Darmstadt). The experiments have been performed with Au+Au, Ni+Ni, C+C at energies between 0.6 and 2.0A GeV [39–48]. One surprising observation in C+C and Ni+Ni collisions [42–44] is that, as a function of the energy difference $\sqrt{s} - \sqrt{s}_{th}$, where $\sqrt{s}_{th}$ is the energy needed to produce the particle (2.5 GeV for K^+ via $pp \to \Lambda K^+ p$ and 2.9 GeV for K^- via $pp \to pp K^- K^+$), the number of K^- balanced the number of K^+ in spite of the fact that in pp collisions the production cross sections close to threshold are two to three orders of magnitude different. This has been interpreted to be a manifestation of the enhancement of the K^+ mass and the reduction of the K^- one in the nuclear medium, which in turn influence the corresponding production thresholds [7,35–38], although a complementary explanation in terms of in-

medium enhanced $\pi\Sigma\rightarrow K^-p$ production has also been given [14]. Another interesting observation is that at incident energies of 1.8 and 1.93A GeV, the K^- and K^+ multiplicities have the same impact parameter dependence [42–44]. Equal centrality dependence for K^+ and K^- and, hence, independence of centrality for the K^-/K^+ ratio have also been observed in Au+Au and Pb+Pb reactions between 1.5A GeV and RHIC energies ($\sqrt{s}=200\text{A GeV}$) [44,49–52]. This independence of centrality is astonishing, since at low energies one expects that as centrality increases—and with it the participating system size and the density probed—the K^-/K^+ ratio should also increase due to the increased reduction of the K^- mass together with the enhancement of the K^+ mass. In fact, the independence of the K^-/K^+ ratio on centrality has often been advocated as signaling the lack of in-medium effects. A recent interesting interpretation of this phenomenon is given in Ref. [53], where it is shown that the K^- are predominantly produced via πY collisions ($Y=\Lambda,\Sigma$) and, hence, the K^- multiplicity is strongly correlated with the K^+ one, since kaons and hyperons are mainly produced together via the reaction $NN\rightarrow KYN$.

Although the transport model calculations show that strangeness equilibration requires times of the order of 40–80 fm/c [54,55], statistical models, which assume chemical and thermal equilibrium and common freeze-out parameters for all particles, are quite successful in describing particle yields including strange particles [56–61]. The kaon and antikaon yields in the statistical models are based on free masses and no medium effects are needed to describe the enhanced in-medium K^-/K^+ ratio or its independence with centrality. The increased value of the K^-/K^+ ratio is simply obtained by choosing a particular set of parameters at freeze-out, the baryonic chemical potential $\mu_B\simeq720$ MeV and the temperature $T\simeq70$ MeV, which also reproduce a variety of particle multiplicity ratios [60,61]. On the other hand, the centrality independence of the K^-/K^+ ratio is automatically obtained in statistical models within the canonical or grand-canonical schemes because the terms depending on the system size drop out [61]. However, as shown by Brown *et al.* in Ref. [62], using the reduced in-medium K^- mass in the statistical model would force, in order to reproduce the experimental value of the K^-/K^+ ratio, a larger value of the chemical potential and hence a larger and more plausible baryonic density for strangeness production. In addition, Brown *et al.* introduce the concept of "broadband equilibration" according to which the K^- mesons and the hyperons are produced in an essentially constant ratio independent of density, hence explaining also the centrality independence of the K^-/K^+ ratio but including medium effects. In essence, the establishment of a broadband relies on the fact that the baryonic chemical potential μ_B increases with density by an amount which coincides roughly with the reduction of the K^- mass. However, as mentioned above, the antikaon properties are very sensitive to the type of model for the $\bar{K}N$ interaction used and of the in-medium effects included. The purpose of the present work is precisely to investigate to which extent the broadband equilibration concept holds when more sophisticated models for the in-medium antikaon

properties are used. We explore within the context of a statistical model what is the behavior of the K^-/K^+ ratio as a function of the nuclear density when the hadrons are dressed, paying special attention to different ways of dressing the antikaons: either treating them as noninteracting or dressing them with an on-shell self-energy, or, finally, considering the complete antikaon spectral density. We use the antikaon self-energy which has been derived within the framework of a coupled-channel self-consistent calculation in symmetric nuclear matter at finite temperature [29], taking as bare meson-baryon interaction the meson-exchange potential of the Jülich group [17]. We will show that the determination of temperature and chemical potential at freeze-out conditions compatible with the experimental value of the K^-/K^+ ratio is very delicate, and depends very strongly on the approximation adopted for the antikaon self-energy.

The paper is organized as follows. In Sec. II, the formalism of the thermal model is described and the different ingredients used in the determination of the off-shell properties of the K^- are given. The results are presented and discussed in Sec. III. Finally, our concluding remarks are given in Sec. IV.

II. FORMALISM

In this section, we present a brief description of the thermal models to account for strangeness production in heavy-ion collisions. The basic hypothesis is to assume that the relative abundance of kaons and antikaons in the final state of relativistic nucleus-nucleus collisions is determined by imposing thermal and chemical equilibrium [56–61,63]. The fact that the number of strange particles in the final state is small requires a strict treatment of the conservation of strangeness and, for this quantum number, one has to work in the canonical scheme. Other conservation laws must also be imposed, such as baryon number and electric charge conservation. Since the number of baryons and charged particles is large, they can be treated in the grand-canonical ensemble. In this way, the conservation laws associated with these other quantum numbers are satisfied on average, allowing for fluctuations around the corresponding mean values.

To restrict the ensemble according to the exact strangeness conservation law, as done in Refs. [56–61], one has to project the grand-canonical partition function $\bar{Z}(T,V,\lambda_B,\lambda_S,\lambda_Q)$ onto a fixed value of strangeness S,

$$Z_S(T,V,\lambda_B,\lambda_Q)=\frac{1}{2\pi}\int_0^{2\pi}d\phi\, e^{-iS\phi}\,\bar{Z}(T,V,\lambda_B,\lambda_S,\lambda_Q),$$

$$(1)$$

where $\lambda_B,\lambda_S,\lambda_Q$ are the baryon, strangeness, and charge fugacities, respectively, and where λ_S stands explicitly for $\lambda_S=e^{i\phi}$.

Only particles with $S=0,\pm1$ are included in the grand-canonical partition function because, in the range of energies achieved at GSI, they are produced with a higher probability than particles with $S=\pm2,\pm3$. The grand-canonical partition function is calculated assuming an independent particle behavior and the Boltzmann approximation for the one-

particle partition function of the different particle species. In principle, one deals with a dilute system, so the independent particle model seems justified. However, medium effects on the particle properties can be relevant. As mentioned in the Introduction, the aim of this paper is to study how the dressing of the hadrons present in the gas, especially the antikaons, affects the observables such as the ratio of kaon and antikaon particle multiplicities, in particular for the conditions of the heavy-ion collisions at SIS/GSI energies.

Within the approximations mentioned above, the grand-canonical partition function reads as follows:

$$\bar{Z}(T,V,\lambda_B,\lambda_S,\lambda_Q) = \exp(N_{S=0} + N_{S=-1}e^{-i\phi} + N_{S=1}e^{i\phi}), \quad (2)$$

where $N_{S=0,\pm1}$ is the sum over one-particle partition functions of all particles and resonances with strangeness $S=0,\pm1$,

$$N_{S=0,\pm1} = \sum_{B_i} Z^1_{B_i} + \sum_{M_j} Z^1_{M_j} + \sum_{R_k} Z^1_{R_k}, \quad (3)$$

$$Z^1_{B_i} = g_{B_i} V \int \frac{d^3p}{(2\pi)^3} e^{-E_{B_i}/T} e^{\mu_{B_i}/T} e^{\mu_{Q(B_i)}/T}, \quad (4)$$

$$Z^1_{M_j} = g_{M_j} V \int \frac{d^3p}{(2\pi)^3} e^{-E_{M_j}/T} e^{\mu_{Q(M_j)}/T}, \quad (5)$$

$$Z^1_{R_k} = g_{R_k} V \int \frac{d^3p}{(2\pi)^3} \int_{m-2\Gamma}^{m+2\Gamma} ds \, e^{-\sqrt{p^2+s}/T}$$

$$\times \frac{1}{\pi} \frac{m\Gamma}{(s-m^2)^2 + m^2\Gamma^2} (e^{\mu_B(R_k)/T}) e^{\mu_Q(R_k)/T}. \quad (6)$$

The expressions $Z^1_{B_i}$ and $Z^1_{M_j}$ indicate the one-particle partition function for baryons and mesons, respectively, while $Z^1_{R_k}$ is the one-particle partition function associated with a baryonic or mesonic resonance. In the latter case, however, the factor $e^{\mu_B(R_k)/T}$ would not be present in Eq. (6). Notice that the resonance is described by means of a Breit-Wigner parametrization. The quantity V is the interacting volume of the system, g_B, g_M, and g_R are spin-isospin degeneracy factors, and μ_B and μ_Q are the baryonic and charge chemical potentials of the system. For Ni+Ni system at SIS energies, μ_Q can be omitted because it is associated with the isospin asymmetry of the system and, in this case, the deviation from the isospin-symmetric case is only 4% (see Ref. [58]). Under these conditions, μ_B coincides with the nucleonic one, μ_N. Since the abundance of nucleons is much larger than the one for the other baryons produced, μ_N can be safely obtained by a purely nucleonic equation of state, as done in the present work. The energies E_B, E_M refer to the in-medium single-particle energies of the hadrons present in the system at a given temperature.

Following Ref. [58], the canonical partition function for total strangeness $S=0$ is

$$Z_{S=0}(T,V,\lambda_B) = \frac{1}{2\pi} \int_0^{2\pi} d\phi$$

$$\times \exp(N_{S=0} + N_{S=-1}e^{-i\phi} + N_{S=1}e^{i\phi}). \quad (7)$$

In this work, as well as in Ref. [59], the small and large volume limits of the particle abundances were studied. These limits were performed to show that the canonical treatment of strangeness in obtaining the particle abundances gives completely different results in comparison to the grand-canonical scheme, demonstrating at the same time that, for the volume considered, the canonical scheme is the appropriate one. The aim of going through these limits again in the following is to remind the reader that, for the specific case of the ratio K^-/K^+, the result is independent of the size of the system and is the same for both the canonical and grand-canonical treatments.

According to statistical mechanics, to compute the number of kaons and antikaons [63] one has to differentiate the partition function with respect to the particle fugacity,

$$N_{K^-(K^+)}$$

$$\equiv \left(\lambda_{K^-(K^+)} \frac{\partial}{\partial\lambda_{K^-(K^+)}} \ln Z_{S=0}(\lambda_{K^-(K^+)}) \right)_{\lambda_{K^-(K^+)}=1}. \quad (8)$$

Expanding $Z_{S=0}$ in the small volume limit, N_{K^-} and N_{K^+} are given by

$$N_{K^+} = g_{K^+} V \int \frac{d^3p}{(2\pi)^3} e^{-E_{K^+}/T}$$

$$\times \left\{ \sum_i g_{B_i} V \int \frac{d^3p}{(2\pi)^3} e^{(-E_{B_i(S=-1)} + \mu_{B_i})/T} \right.$$

$$\left. + \sum_j g_{M_j} V \int \frac{d^3p}{(2\pi)^3} e^{-E_{M_j(S=-1)}/T} + \sum_k Z^1_{R_{k(S=-1)}} \right\},$$

$$N_{K^-} = g_{K^-} V \int \frac{d^3p}{(2\pi)^3} e^{-E_{K^-}/T}$$

$$\times \left\{ \sum_j g_{M_j} V \int \frac{d^3p}{(2\pi)^3} e^{-E_{M_j(S=+1)}/T} + \sum_k Z^1_{R_{k(S=+1)}} \right\}, \quad (9)$$

where antibaryons have not been considered because the ratio $\bar{B}/B = e^{-2\mu_B/T}$ is negligibly small at GSI/SIS colliding energies, where B and $\bar{B}$ represent the number of baryons and antibaryons, respectively. The expression for N_{K^+} (N_{K^-}) indicates that the number of K^+ (K^-) has to be balanced with all particles and resonances with $S=-1$ ($S=1$). It can be observed from Eq. (9) that the ratio $K^-/K^+ \equiv N_{K^-}/N_{K^+}$ in the canonical ensemble does not depend on the volume because it cancels out exactly.

At the other extreme, i.e., in the thermodynamic limit (large volumes), since it is known that the canonical treatment is equivalent to the grand-canonical one, one can compute the ratio explicitly from the grand-canonical partition function $\bar{Z}(T,V,\lambda_B,\lambda_S)$,

$$\ln \bar{Z}(T,V,\lambda_B,\lambda_S) = \lambda_S Z_{K^+}^1 + \frac{1}{\lambda_S} Z_{K^-}^1 + \lambda_B \frac{1}{\lambda_S} Z_{B,S=-1}^1$$

$$+ \lambda_S Z_{M,S=+1}^1 + \frac{1}{\lambda_S} Z_{M,S=-1}^1, \quad (10)$$

where $Z_{B,S=\pm 1}^1$ ($Z_{M,S=\pm 1}^1$) is the sum of one-particle partition functions for baryons (mesons) with $S=\pm 1$. Then, by imposing strangeness conservation on average,

$$\langle S \rangle = \lambda_S \frac{\partial}{\partial \lambda_S} \ln \bar{Z} = 0, \quad (11)$$

one can easily obtain λ_S,

$$\lambda_S^2 = \frac{Z_{K^-}^1 + \lambda_B Z_{B,S=-1}^1 + Z_{M,S=-1}^1}{Z_{K^+}^1 + Z_{M,S=+1}^1}. \quad (12)$$

Therefore, from

$$\langle N_{K^+} \rangle = \lambda_S Z_{K^+}^1,$$

$$\langle N_{K^-} \rangle = \frac{1}{\lambda_S} Z_{K^-}^1, \quad (13)$$

one obtains the ratio

$$\frac{K^-}{K^+} = \frac{Z_{K^-}^1}{Z_{K^+}^1} \frac{Z_{K^+}^1 + Z_{M,S=+1}^1}{Z_{K^-}^1 + \lambda_B Z_{B,S=-1}^1 + Z_{M,S=-1}^1}. \quad (14)$$

The condition $\langle S \rangle = 0$ and dealing with strange particles of $S=0,\pm 1$ make the ratio independent of the volume.

Although the expression obtained is the same as that from the canonical ensemble in the small volume limit, the proof that the ratio K^-/K^+ is independent of the volume has to be obtained from a general intermediate size situation. This was shown to be the case in Ref. [60], where expanding $Z_{S=0}(T,V,\lambda_B)$ of Eq. (7) in power series, it was expressed as $Z_{S=0} = Z_0 I_0(x_1)$, where Z_0 is the partition function that includes all particles and resonances with $S=0$, $I_0(x_1)$ is the modified Bessel function, and $x_1 = 2\sqrt{N_{S=1}N_{S=-1}}$. The computed K^-/K^+ ratio gave precisely the same expression as those given here for small [Eq. (9)] and large [Eq. (14)] volumes. Therefore, as noted in Ref. [59], the K^-/K^+ ratio is independent of the volume and, consequently, independent of whether it is calculated in the canonical or grand-canonical schemes.

In-medium effects in K^-/K^+ ratio at finite T

In this section, we study how the in-medium modifications of the properties of the hadrons at finite temperature affect the value of the K^-/K^+ ratio, focusing our attention on the properties of the antikaons in hot and dense matter. For consistency with previous papers, we prefer to compute the inverse ratio K^+/K^-. As it was mentioned before, the number of K^- (K^+) has to be balanced by particles and resonances with $S=+1$ ($S=-1$) in order to conserve strangeness exactly. For balancing the number of K^+, the main contribution in the $S=-1$ sector comes from the Λ and Σ hyperons and, in a smaller proportion, from the K^- mesons. In addition, the effect of the $\Sigma^*(1385)$ resonance is also considered because it is comparable to that of the K^- mesons. On the other hand, the number of K^- is balanced only by the presence of K^+. Then, we can write the K^+/K^- ratio as

$$\frac{K^+}{K^-} \equiv \frac{N_{K^+}}{N_{K^-}} = \frac{Z_{K^+}^1 (Z_{K^-}^1 + Z_\Lambda^1 + Z_\Sigma^1 + Z_{\Sigma^*}^1)}{Z_{K^-}^1 Z_{K^+}^1}$$

$$= 1 + \frac{Z_\Lambda^1 + Z_\Sigma^1 + Z_{\Sigma^*}^1}{Z_{K^-}^1}, \quad (15)$$

where the Z's indicate the different one-particle partition functions for K^-, K^+, Λ, Σ, and Σ^*, and for baryons, they now contain the corresponding fugacity. It is clear from Eq. (15) that the relative abundance of Λ, Σ, and Σ^* baryons with respect to that of K^- mesons determines the value of the ratio.

In order to introduce the in-medium and temperature effects, the particles involved in the calculation of the ratio are dressed according to their properties in the hot and dense medium in which they are embedded. For the Λ and Σ hyperons, the partition function

$$Z_{\Lambda,\Sigma}^1 = g_{\Lambda,\Sigma} V \int \frac{d^3 p}{(2\pi)^3} e^{(-E_{\Lambda,\Sigma} + \mu_B)/T} \quad (16)$$

is constructed using a mean-field dispersion relation for the single-particle energies:

$$E_{\Lambda,\Sigma} = \sqrt{m_{\Lambda,\Sigma}^2 + p^2} + U_{\Lambda,\Sigma}(\rho). \quad (17)$$

For $U_\Lambda(\rho)$, we take the parametrization of Ref. [64], $U_\Lambda(\rho) = -340\rho + 1087.5\rho^2$. For $U_\Sigma(\rho)$, we take a repulsive potential, $U_\Sigma(\rho) = 30\rho/\rho_0$, extracted from the analysis of Σ atoms and Σ-nucleus scattering [65,66], where $\rho_0 = 0.17$ fm^{-3} is the saturation density of symmetric nuclear matter. A repulsive Σ potential is compatible with the absence of any bound state or narrow peaks in the continuum in a recent Σ-hypernuclear search done at BNL [67]. The $\Sigma^*(1385)$ resonance is described by a Breit-Wigner shape,

$$Z_{\Sigma^*}^1 = g_{\Sigma^*} V \int \frac{d^3 p}{(2\pi)^3} \int ds \, e^{-\sqrt{p^2 + s}/T}$$

$$\times \frac{1}{\pi} \frac{m_{\Sigma^*}\Gamma}{(s - m_{\Sigma^*}^2)^2 + m_{\Sigma^*}^2\Gamma^2} e^{\mu_B/T}, \quad (18)$$

with $m_{\Sigma*} = 1385$ MeV and $\Gamma = 37$ MeV, where $\sqrt{s}$ is integrated from $m_{\Sigma*} - 2\Gamma$ to $m_{\Sigma*} + 2\Gamma$.

In the case of K^+, we take

$$Z^1_{K^+} = g_{K^+} V \int \frac{d^3 p}{(2\pi)^3} e^{-E_{K^+}/T}, \qquad (19)$$

$$E_{K^+} = \sqrt{m^2_{K^+} + p^2} + U_{K^+}(\rho), \qquad (20)$$

where $U_{K^+}(\rho) = 32\rho/\rho_0$ is obtained from a $t\rho$ approximation, as discussed in Refs. [10,68]. One could also take for the kaon potential the recent experimental value of 20 MeV at ρ_0 [69]. However, we note that in the present approach the properties of the kaons do not play a direct role in the determination of the K^+/K^- ratio. The reason is that the negative strangeness of the antikaons is balanced only with $S = +1$ kaons and, as seen in Eq. (15), the corresponding partition function cancels out in performing the ratio.

A particular effort has been invested in studying the antikaon properties in the medium, since the $\bar{K}N$ has a particularly rich structure due to the presence of the $\Lambda(1405)$ resonance [12–15]. The antikaon optical potential in hot and dense nuclear matter has recently been obtained [29] within the framework of a coupled-channel self-consistent calculation taking, as bare meson-baryon interaction, the meson-exchange potential of the Jülich group [17]. In order to understand the influence of the in-medium antikaon properties on the K^+/K^- ratio, two different prescriptions for the single-particle energy of the antikaons have been considered.

First, the so-called on-shell approximation to the antikaon single-particle energy has been adopted. The antikaon partition function in this approach reads

$$Z^1_{K^-} = g_{K^-} V \int \frac{d^3 p}{(2\pi)^3} e^{-E_{K^-}/T},$$

$$E_{K^-} = \sqrt{m^2_{K^-} + p^2} + U_{\bar{K}}(T,\rho,E_{K^-},p), \qquad (21)$$

where $U_{\bar{K}}(T,\rho,E_{K^-},p)$ is the $\bar{K}$ single-particle potential in the Brueckner-Hartree-Fock approach given by

$$U_{\bar{K}}(T,\rho,E_{K^-},p)$$
$$= \text{Re} \int d^3 k\, n(k,T) \langle \bar{K}N | G_{\bar{K}N \to \bar{K}N}(\Omega = E_N + E_{\bar{K}},T) | \bar{K}N \rangle,$$
$$(22)$$

which is built from a self-consistent effective $\bar{K}N$ interaction in nuclear symmetric matter, averaging over the occupied nucleonic states according to the Fermi distribution at a given temperature, $n(k,T)$.

The second approach incorporates the complete energy-and-momentum dependent $\bar{K}$ self-energy

$$\Pi_{\bar{K}}(T,\rho,\omega,p) = 2\sqrt{p^2 + m^2_{\bar{K}}} U_{\bar{K}}(T,\rho,\omega,p), \qquad (23)$$

via the corresponding $\bar{K}$ spectral density

$$S_{\bar{K}}(T,\rho,\omega,p) = -\frac{1}{\pi} \text{Im}\, D_{\bar{K}}(T,\rho,\omega,p), \qquad (24)$$

where

$$D_{\bar{K}}(T,\rho,\omega,p) = \frac{1}{\omega^2 - p^2 - m^2_{\bar{K}} - \Pi_{\bar{K}}(T,\rho,\omega,p)} \qquad (25)$$

stands for the $\bar{K}$ propagator. In this case, the $\bar{K}$ partition function reads

$$Z^1_{K^-} = g_{K^-} V \int \frac{d^3 p}{(2\pi)^3} \int ds\, S_{\bar{K}}(T,\rho,\omega = \sqrt{s},p) e^{-\sqrt{s}/T}, \qquad (26)$$

where $s = \omega^2$.

We note, however, that only the s-wave contribution of the Jülich $\bar{K}N$ interaction has been kept. The reason is that this potential presents some shortcomings in the $L = 1$ partial wave, which manifest themselves especially in the low-energy region of the $\bar{K}$ self-energy. Specifically, the Λ and Σ poles of the $\bar{K}N$ T matrix come out lower about 100 MeV than the physical values and, consequently, the corresponding strength in the antikaon spectral function due to hyperon-hole excitations appears at too low energies, a region very important for the calculation we are conducting here. In addition, the role of the $\Sigma^*(1385)$ pole, which lies below the $\bar{K}N$ threshold, is not included in the Jülich $\bar{K}N$ interaction. In order to overcome these problems, we have added to our $\bar{K}$ self-energy the p-wave contribution as calculated in Ref. [68]. In this model, the p-wave self-energy comes from the coupling of the $\bar{K}$ meson to hyperon-hole (YN^{-1}) excitations, where Y stands for Λ, Σ, and Σ^*. In symmetric nuclear matter at $T = 0$, this self-energy reads

$$\Pi^p_{\bar{K}}(\rho,\omega,\vec{p}) = \frac{1}{2}\left(\frac{g_{N\Lambda\bar{K}}}{2M}\right)^2 \vec{p}^{\,2} f^2_\Lambda \mathcal{U}_\Lambda(\rho,\omega,\vec{p})$$
$$+ \frac{3}{2}\left(\frac{g_{N\Sigma\bar{K}}}{2M}\right)^2 \vec{p}^{\,2} f^2_\Sigma \mathcal{U}_\Sigma(\rho,\omega,\vec{p})$$
$$+ \frac{1}{2}\left(\frac{g_{N\Sigma*\bar{K}}}{2M}\right)^2 \vec{p}^{\,2} f^2_{\Sigma*} \mathcal{U}_{\Sigma*}(\rho,\omega,\vec{p}). \quad (27)$$

The quantities $g_{N\Lambda\bar{K}}$, $g_{N\Sigma\bar{K}}$, and $g_{N\Sigma*\bar{K}}$ are the $N\Lambda\bar{K}$, $N\Sigma\bar{K}$, and $N\Sigma^*\bar{K}$ coupling constants, while f_Λ, f_Σ, $f_{\Sigma*}$ are the Λ, Σ, Σ^* relativistic recoil vertex corrections and $\mathcal{U}_\Lambda$, $\mathcal{U}_\Sigma$, $\mathcal{U}_{\Sigma*}$ the Lindhard functions at $T = 0$. For more details, see Ref. [68]. The relevance of this low-energy region makes it advisable to extend this p-wave contribution to finite temperature.

The hyperon-hole Lindhard functions at finite temperature are easily obtained from the Δ-hole one given in Eq. (A16) of Ref. [29], by ignoring, due to strangeness conservation, the crossed-term contribution. The spin-isospin degeneracy factors and coupling constants need to be accommodated to
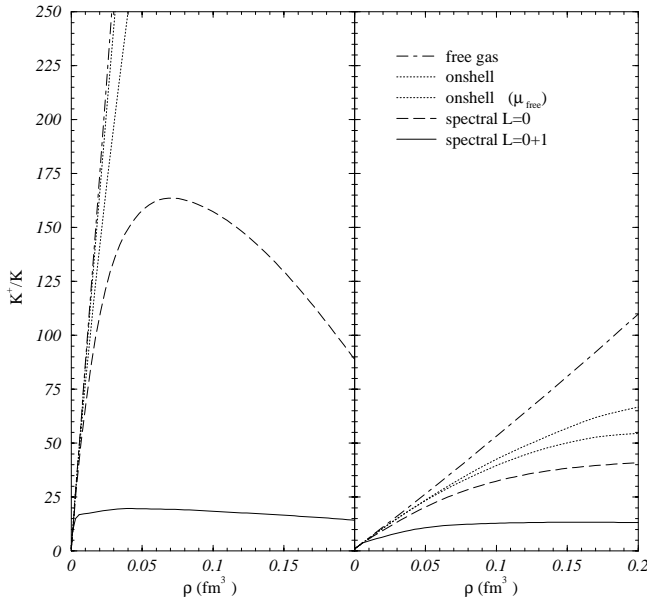
FIG. 1. K^+/K^- ratio as a function of the density for $T = 50$ MeV (left panel) and $T = 80$ MeV (right panel) calculated in different approaches: the free Fermi gas (dot-dashed line), on-shell self-energies (dotted line), on-shell self-energies with μ from a free (noninteracting) Fermi gas (thin dotted line), dressing the K^- with its single-particle spectral function, with the $L = 0$ contribution (long-dashed line) and taking into account the additional $L = 1$ partial wave (solid line).

the notation used in Eq. (27) and this amounts to replacing $(2/3)(f_\Lambda^*/f_N)$ by $3/2$. Finally, the width Γ in Eq. (A16) of Ref. [29] is taken to zero, not only for the stable Λ and Σ hyperons but also, for simplicity, for the Σ^* hyperon, which allows one to obtain the imaginary part of the Lindhard function analytically.

III. RESULTS

In this section, we discuss the effects of dressing the K^- mesons in hot and dense nuclear matter on the K^-/K^+ ratio around the value found in Ni+Ni collisions at an energy of 1.93A GeV. A preliminary study was already reported in Ref. [70]. As previously mentioned, we prefer to discuss the results for the inverted ratio K^+/K^-.

The K^+/K^- ratio is shown in Fig. 1 as a function of density at two given temperatures, $T = 50$ and 80 MeV, calculated for the three ways of dressing of the K^-: free (dot-dashed lines), the on-shell or mean-field approximation of Eq. (21) (dotted lines), and using the $\bar{K}$ spectral density including s-wave (long-dashed lines) or both s-wave and p-wave contributions (solid lines). The two chosen temperatures roughly delimit the range of temperatures which have been claimed to reproduce, in the framework of the thermal model, not only the K^+/K^- ratio but also all the other particle ratios involved in the Ni+Ni collisions at SIS energies [58,59].

Since the baryonic chemical potential μ_B grows with density, the factor $e^{\mu_B/T}$ in the partition functions of Eqs. (16)

and (18) allows one to understand why the ratio increases so strongly with density in the free gas approximation (dot-dashed lines). The same is true when the particles are dressed. In this case, however, the K^- feels an increasing attraction with density which tends to compensate the variation of μ_B and the curves bend down after the initial increase. This effect is particularly notorious when the full $\bar{K}$ spectral density is used. The results are in qualitative agreement with the broadband equilibration notion introduced by Brown *et al.* [62]. However, in this present model, the gain in binding energy in the on-shell approximation for K^- (thick dotted line in Fig. 1) when the density grows does not completely compensate the increase of μ_B, as was the case in Ref. [62]. To illustrate this fact, we note that the variation of the K^- single-particle energy at zero momentum at $T = 70$ MeV changes in our model [29] from 434 MeV to 375 MeV when the density grows from $1.2\rho_0$ to $2.1\rho_0$, while μ_B changes from 873 MeV to 962 MeV. Therefore, the relevant quantity to understand the behavior of the K^+/K^- ratio with density in the on-shell approximation, i.e., the sum of μ_B and E_{K^-} (see Eq. (6) of Ref. [62]), suffers in our model a variation of about 30 MeV. On the other hand, the model of Ref. [62] assumed a slower variation of μ_B, from 860 MeV to 905 MeV, which was almost canceled by the change of E_{K^-} from 380 MeV to 332 MeV, giving therefore a practically density independent ratio. We note that our chemical potential is derived from a nucleonic energy spectrum obtained in a Walecka σ-ω model, using density dependent scalar and vector coupling constants fitted to reproduce Dirac-Brueckner-Hartree-Fock calculation (see Table 10.9 in Ref. [71]).

The results obtained in the present microscopic calculation show that the broadband equilibration only shows up clearly when the full spectral function is used (solid line in Fig. 1). After an increase at low densities, the K^+/K^- ratio remains constant at intermediate and high densities. The use of the spectral density implicitly amounts to an additional gain in binding energy for the antikaons and, as density increases, it compensates rather well the variation of μ_B.

To understand the origin of this additional effective attraction when the full spectral density is used, we show in Fig. 2 the two functions that contribute to the integral over the energy in the definition of the K^- partition function [Eq. (26)], namely, the Boltzmann factor $e^{-\sqrt{s}/T}$ and the K^- spectral functions including $L = 0$ (long-dashed line) and $L = 0 + 1$ (solid line) components of the $\bar{K}N$ interaction, for a momentum $q = 500$ MeV at $\rho = 0.17$ fm^{-3} and $T = 80$ MeV. As it is clearly seen in the figure, the overlap of the Boltzmann factor with the quasiparticle peak of the K^- spectral function is small for this momentum. It is precisely the overlap with the strength in the low-energy region that acts as a source of attraction in the contribution to the K^- partition function. This effect is particularly pronounced when the p waves are included, due to the additional low-energy components in the spectral function coming from the coupling of the K^- meson to hyperon-hole (YN^{-1}) excitations, where Y stands for Λ, Σ, and Σ^*. Assigning these low-energy components to real antikaons in the medium is not clear, since one should interpret them as representing the production of hyperons through
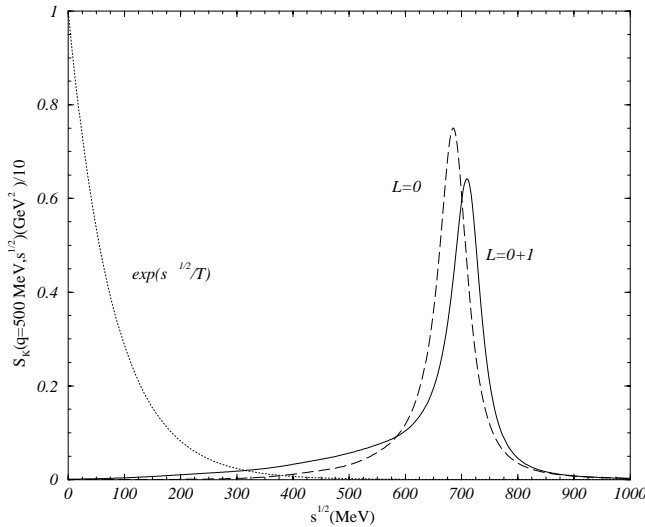
FIG. 2. The Boltzmann factor (dotted line) and the K^- spectral function, including s-wave (dashed line) or s- and p-wave (solid line) components of the $\bar{K}N$ interaction, as functions of the energy, for a momentum $q=500$ MeV at saturation density and temperature $T=80$ MeV.

$\bar{K}N \rightarrow Y$ conversion. While this is certainly true, it may also happen that, once these additional hyperons are present in the system, they can subsequently interact with fast nonstrange particles (pions, nucleons) to create new antikaons. A clear interpretation on what fraction of the low-energy strength will emerge as antikaons at freeze-out is certainly an interesting question and its investigation will be left here for forthcoming work.

Once the integral over the energy is performed, the determination of the K^- partition function still requires an integral over the momentum. The integrand as a function of momentum is plotted in Fig. 3 for the same density and temperature than in the previous figure. As expected, the integrand is larger when the full spectral density is considered. In this case, the K^- partition function is enhanced and therefore the K^+/K^- ratio is smaller than that in the on-shell approximation and also in the case where only the $L=0$ contributions to the spectral density are used. Notice the behavior at large q, which decays very quickly in the on-shell approximation but has a long tail for the $L=0+1$ spectral density originated from the coupling of the K^- meson to YN^{-1} configurations.

Another aspect that we want to consider is how the dressing of the Σ hyperon affects the value of the ratio. In Fig. 4, the value of the K^+/K^- ratio at $T=50$ MeV is shown as a function of density for different situations. In all calculations displayed in the figure, the partition function associated with K^- has been obtained using the full K^- spectral density. The dotted line corresponds to the case where only the Λ hyperons, dressed with the attractive mean-field potential given in the preceding section, are included to balance strangeness. When the Σ hyperon is incorporated with a moderately attractive potential of the type $U_\Sigma = -30\rho/\rho_0$ MeV, the K^+/K^- ratio is enhanced substantially (dashed line). This enhancement is more moderate when one uses the repulsive
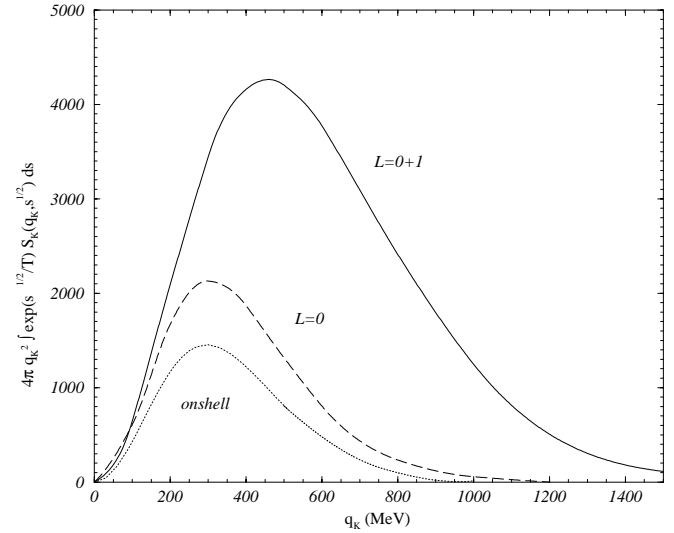

FIG. 3. The integrand which defines the K^- partition function [Eq. (26)] as a function of momentum, at saturation density and $T=80$ MeV, for different approaches: on-shell prescription (dotted line), using the K^- spectral function with the $L=0$ components of the $\bar{K}N$ interaction (long-dashed line) and including also the $L=1$ partial waves (solid line).

potential $U_\Sigma = +30\rho/\rho_0$ instead (dot-dashed line). Finally, the additional contribution of the Σ^* resonance produces only a small increase of the ratio (solid line) due to its higher mass. We have checked that heavier strange baryonic or mesonic resonances do not produce visible changes in our results. Notice also that, although the ratios obtained with both prescriptions for the mean-field potential of the Σ meson differ appreciably, the present uncertainties in the ratio
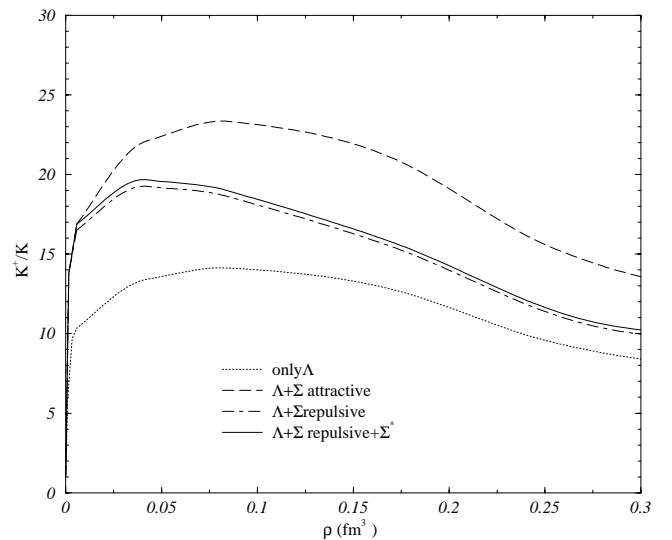

FIG. 4. The K^+/K^- ratio as a function of density at $T=50$ MeV. The dotted line shows the results when only the Λ hyperons are considered in the determination of the ratio. The dashed (dot-dashed) line includes also the contribution of the Σ hyperon dressed with an attractive (repulsive) mean-field potential. The solid line includes the effect of the Σ^* resonance.
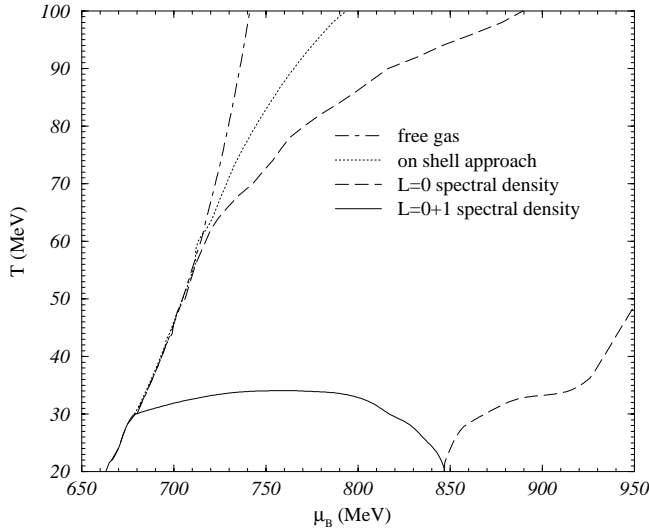
FIG. 5. Relation between the temperature and the baryochemical potential of hadronic matter produced in heavy-ion collisions for fixed K^+/K^- ratio of 30, calculated within different approaches as discussed in the text.

would not permit to discriminate between them.

In the framework of the statistical model, one obtains a relation between the temperature and the chemical potential of the hadronic matter produced in the heavy-ion collisions by fixing the value of the K^-/K^+ ratio which was measured for Ni+Ni collisions at GSI to be on the average $K^-/K^+ = 0.031 \pm 0.005$ [44]. We compare our results with a corresponding inverse ratio of $K^+/K^- = 30$ in the following. The temperatures and chemical potentials compatible with that ratio are shown in Fig. 5 for different approaches. The dot-dashed line stands for a free gas of hadrons, similar to the calculations reported in Refs. [58,59]. The dotted line shows the $T(\mu)$ curve obtained with the on-shell or mean-field approximation [see Eqs. (21) and (22)], while the dashed and solid lines correspond to the inclusion of the off-shell properties of the K^- self-energy by using its spectral density [Eqs. (23), (24) and (26)], including $L=0$ or $L=0+1$ components, respectively.

In the free gas limit, the temperatures compatible with a ratio $K^+/K^- = 30$ imply a narrow range of values for the baryonic chemical potentials, namely, $\mu_B \in [665,740]$ MeV for temperatures in the range of 20–100 MeV. These values translate into density ranges of $\rho \in [6 \times 10^{-7}\rho_0, 0.9\rho_0]$.

As it can be seen from the dotted line in Fig. 5, the attractive mean-field potential of the antikaons compensates the effect of increasing baryochemical potential μ_B. As a consequence, the density at which the freeze-out temperature compatible with the measured ratio takes place also grows. But this attraction is not enough to get the same K^+/K^- ratio for a substantially broader range of density compared to the free case. So we do not see a clear indication of broadband equilibration in our self-consistent mean-field calculation in contrast to the results of Brown, Rho, and Song [62].

The influence of the antikaon dressing on the ratio is much more evident when the spectral density is employed

(long-dashed and solid lines). From the preceding discussions, it is easy to understand that the low-energy behavior of the spectral density enhances the K^- contribution to the ratio, having a similar role as an attractive potential and, hence, the value of μ_B compatible with a ratio at a given temperature increases. Moreover, due to the bending of the K^+/K^- ratio with density and its evolution with temperature observed in Fig. 1, it is clear that there will be a maximum value of T compatible with a given value of the ratio. Below this maximum temperature, there will be two densities or, equivalently, two chemical potentials compatible with the ratio. For example, the ratio $K^+/K^- = 30$ will in fact not be realized with the temperatures of $T=50$ MeV and $T=80$ MeV displayed in Fig. 1, if the antikaon is dressed with the spectral density containing $L=0$ and $L=1$ components. As shown in Fig. 5, only temperatures lower than 34 MeV are compatible with ratio values of 30.

We note that the flat regions depicted by the solid lines in Fig. 5 could be considered to be in correspondence with the notion of broadband equilibration of Brown *et al.* [62], in the sense that a narrow range of temperatures and a wide range of densities are compatible with a particular value of the K^+/K^- ratio. Nevertheless, the temperature range is too low to be compatible with the measured slope parameter of the pion spectra. Explicitly, for $K^+/K^- = 30$, we observe a nearly constant ratio observed in the range of 30–34 MeV covering a range of chemical potentials in between 680 and 815 MeV which translates into a density range $\rho \in [1.5 \times 10^{-4}\rho_0, 0.02\rho_0]$. Note that in this case, we can hardly speak of a broadband equilibration in the sense of that introduced by Brown, Rho, and Song in Ref. [62], where a ratio $K^+/K^- = 30$ holds over a large range of densities in between $\frac{1}{4}\rho_0$ and $2\rho_0$ for $T=70$ MeV. However, as we indicated at the beginning of this section, this result was obtained in the framework of a mean-field model and our equivalent on-shell results (dashed lines in Figs. 1 and 5), based on a stronger variation of the μ_B with density and on a less attractive $U_{\bar{K}}$, seem to be very far from producing the broadband equilibration behavior.

As pointed out before, our nucleon chemical potential is obtained in the framework of a relativistic model and varies with density more strongly than that used in Ref. [62], which shows values close to those for a free Fermi gas. If we now calculate the K^+/K^- ratio using a $\mu_B(\rho,T)$ for a free (non-interacting) system in the on-shell approximation, we obtain the thin dotted line in Fig. 1. At $T=80$ MeV, we now observe a tendency of a broadband equilibration but for ratios higher than 30, of around 50. This is connected to the particular on-shell potential of the antikaon which, in our self-consistent procedure, turns to be moderately attractive. Only if the attraction was larger would the broadband be realized in this on-shell picture for smaller values of the ratio as found by Brown *et al.* [62].

Figure 6 shows the K^+/K^- ratio for the full model calculation as a contour plot for different temperatures and baryochemical potentials. We note that the ratio is substantially lower at the temperature and density range of interest, being more likely around 15 or so for a moderately large region of baryochemical potential. Note that this reduced ratio trans-
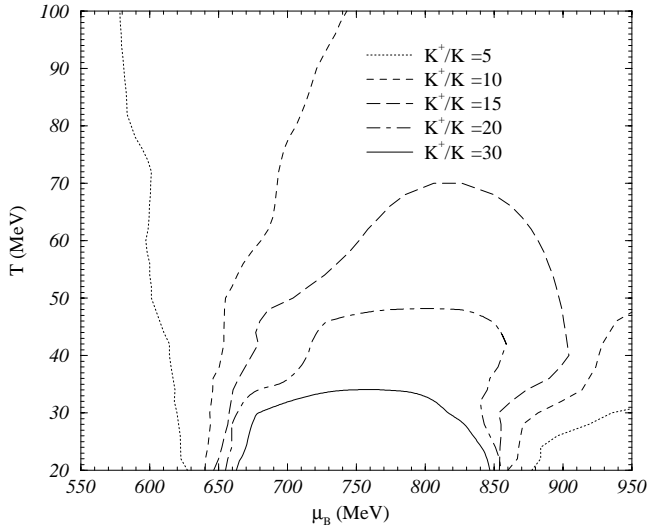
FIG. 6. The K^+/K^- ratio plotted for the full spectral density of the K^- as a contour plot for different temperatures and baryochemical potentials.

lates into an overall enhanced production of K^- by a factor 2 compared to the experimentally measured value. At pion freeze-out, the medium can hold twice as many K^- as needed to explain the measured enhanced production of K^- if one considers the full spectral features of the K^- in the medium. We stress again that this enhancement is not due to an increased attraction in the sense of a mean-field calculation. It is a consequence of the additional strength of the spectral function at low energies, which emerges when taking into account p-wave hyperon-hole excitations. The Boltzmann factor amplifies the contribution of the low-energy region of the spectral function so that these excitations are becoming the main reason for the overall enhanced production of the K^- in the medium.

IV. CONCLUSIONS

We have studied, within the framework of a statistical model, the influence of considering the modified properties in hot and dense matter of the hadrons involved in the determination of the K^-/K^+ ratio produced in heavy-ion collisions at SIS/GSI. We have focused our attention on incorporating the effects of the antikaon self-energy, which was derived within the framework of a self-consistent coupled-channel calculation taking, as bare interaction, the meson-exchange potential of the Jülich group for the s-wave and adding the p-wave components of the Yh excitations, with $Y=\Lambda,\Sigma,\Sigma*$.

It is found that the determination of the temperature and chemical potential at freeze-out conditions compatible with the ratio K^-/K^+ is very delicate and depends very strongly on the approximation adopted for the antikaon self-energy. The effect of dressing the K^- with a spectral function including both s- and p-wave components of the $\bar{K}N$ interaction lowers considerably the effective temperature while increasing the chemical potential μ_B up to 850 MeV, compared to calculations for a noninteracting hadron gas.

When the free or on-shell properties of the antikaon are considered, the ratio at a given temperature shows a strong dependence on the density. This is in contrast with the broadband equilibration advocated by Brown *et al.* [62], which was established, in the context of a mean-field picture, through a compensation between the increased attraction of the mean-field $\bar{K}$ potential as density grows with the increase in the baryon chemical potential. Our mean-field properties do not achieve such a compensation due to a stronger increase of the nucleon chemical potential μ_B with density.

When taking into account the full features of the spectral function of the K^- via hyperon-hole excitations, we find that the K^-/K^+ ratio exhibits broadband equilibration. Nevertheless, the ratio is even in excess of the measured ratio at temperatures which are deduced from the slope parameter for pions. The incompatibility with the experimentally measured ratio can be resolved in several ways. First, the spectral function has too much strength below threshold and there is no broadband equilibration. Second, the simple statistical ansatz cannot be used for a medium modified K^-.

Admitting the plausibility of our approach, one would still need, in order to see the particle ratios of the medium, to assume an instantaneous substantial change of the spectral function from the in-medium one to the free one at freeze-out, i.e., it must be fast enough so that inelastic collisions are not possible anymore. If that process is too slow, particle ratios will be adjusted accordingly yielding a final ratio which is compatible with that of a free gas of noninteracting particles. The K^- interacts quite strongly with the medium, transforming nucleons to hyperons and pions. If that inelastic process ceases later than the ones for pions, the corresponding particle ratios will be fixed at a different value of temperature and baryochemical potential than that deduced from the slope of the transverse mass spectrum of the pions. Indeed, different slope parameters for K^+ and K^- have been measured in heavy-ion experiments at GSI by the KaoS Collaboration [72] where the slope parameter for the antikaons is significantly lower than that for kaons. In addition, K^- are emitted isotropically for central collisions, while there is a strong forward/backward enhancement in the angular distribution for produced K^+ [23]. From microscopical transport models, it is also well known that the antikaons freeze-out much later than kaons due to their substantially shorter mean-free path (see, e.g., Ref. [73]). These observations indicate that the statistical description of subthreshold antikaon production has to be taken with care. We note that the different slope parameters for kaons and antikaons can indeed be attributed to medium effects, especially to a sizable attraction in the medium felt by the antikaons (see, e.g., Refs. [74,75]).

The question how the antikaon gets on shell and what fraction of the antikaon strength emerges as real antikaons are interesting ones. This investigation is outside the scope of the present study and is left to be addressed in forthcoming work. We note, however, that the first question is addressed recently in an off-shell transport model simulation and refer the interested reader to Ref. [76] which uses essentially the same spectral function for antikaons as in the present work. There it is shown that the antikaon spectral function reaches

the vacuum asymptotically. The necessary energy to lift the in-medium antikaons to the free one is taken from the transverse expansion of the surrounding matter. Most importantly for our discussion outlined here, the transport model simulation demonstrates that the expansion is sufficiently fast to preserve the in-medium information of antikaons and shows a significant different slope parameter for kaons and antikaons.

[1] G.E. Brown and M. Rho, Phys. Rep. **363**, 85 (2002).

[2] J. Wambach, Nucl. Phys. **A699**, 10 (2002).

[3] U. Mosel, Prog. Part. Nucl. Phys. **42**, 163 (1999).

[4] H. Heiselberg and M. Hjorth-Jensen, Phys. Rep. **328**, 237 (2000).

[5] D.B. Kaplan and A.E. Nelson, Phys. Lett. B **175**, 57 (1986); **179**, 409(E) (1986).

[6] G.E. Brown and H.A. Bethe, Astrophys. J. **423**, 659 (1994); Nucl. Phys. **A567**, 937 (1994).

[7] G.Q. Li, C.-H. Lee, and G. Brown, Phys. Rev. Lett. **79**, 5214 (1997).

[8] A. Ramos, J. Schaffner-Bielich, and J. Wambach, in *Physics of Neutron Star Interiors*, edited by D. Blaschke, N. K. Glendenning, and A. Sedrakian, Lecture Notes in Physics Vol. 578 (Springer, New York, 2001), p. 175, and references therein.

[9] V. Koch, Phys. Lett. B **337**, 7 (1994).

[10] N. Kaiser, P.B. Siegel, and W. Weise, Nucl. Phys. **A594**, 325 (1995); N. Kaiser, T. Waas, and W. Weise, *ibid.* **A612**, 297 (1997).

[11] E. Friedman, A. Gal, and C.J. Batty, Nucl. Phys. **A579**, 518 (1994).

[12] M. Lutz, Phys. Lett. B **426**, 12 (1998).

[13] A. Ramos and E. Oset, Nucl. Phys. **A671**, 481 (2000).

[14] J. Schaffner-Bielich, V. Koch, and M. Effenberger, Nucl. Phys. **A669**, 153 (2000).

[15] L. Tolós, A. Ramos, A. Polls, and T.T.S. Kuo, Nucl. Phys. **A690**, 547 (2001).

[16] E. Oset and A. Ramos, Nucl. Phys. **A635**, 99 (1998).

[17] A. Müller-Groeling, K. Holinde, and J. Speth, Nucl. Phys. **A513**, 557 (1990).

[18] S. Hirenzaki, Y. Okumura, H. Toki, E. Oset, and A. Ramos, Phys. Rev. C **61**, 055205 (2000).

[19] A. Baca, C. García-Recio, and J. Nieves, Nucl. Phys. **A673**, 335 (2000).

[20] A. Cieplý, E. Friedman, A. Gal, and J. Mareš, Nucl. Phys. **A696**, 173 (2001).

[21] H. Oeschler, J. Phys. G **28**, 1787 (2002).

[22] P. Senger, Acta Phys. Pol. B **31**, 2313 (2000); Nucl. Phys. **A685**, 312 (2001).

[23] C. Sturm *et al.*, J. Phys. G **28**, 1895 (2002).

[24] J. Caro-Ramon, N. Kaiser, S. Wetzel, and W. Weise, Nucl. Phys. **A672**, 249 (2000).

[25] M.F.M. Lutz and E.E. Kolomeitsev, Nucl. Phys. **A700**, 193 (2002).

[26] D. Jido, E. Oset, and A. Ramos, Phys. Rev. C **66**, 055203 (2002).

[27] M.F.M. Lutz and C.L. Korpa, Nucl. Phys. **A700**, 309 (2002).

[28] E.E. Kolomeitsev and D.N. Voskresensky, nucl-th/0211052.

[29] L. Tolós, A. Ramos, and A. Polls, Phys. Rev. C **65**, 054907 (2002).

[30] C.M. Ko, Q. Li, and R. Wang, Phys. Rev. Lett. **59**, 1084 (1987).

[31] S. Teis, W. Cassing, M. Effenberger, A. Hombach, U. Mosel, and G. Wolf, Z. Phys. A **356**, 421 (1997).

[32] M. Effenberger, E.L. Bratkovskaya, W. Cassing, and U. Mosel, Phys. Rev. C **60**, 027601 (1999).

[33] C. Fuchs, A. Faessler, E. Zabrodin, and Y.M. Zheng, Phys. Rev. Lett. **86**, 1974 (2001).

[34] C. Hartnack *et al.*, Eur. Phys. J. A **1**, 151 (1998).

[35] W. Cassing, E.L. Bratkovskaya, U. Mosel, S. Teis, and A. Sibirtsev, Nucl. Phys. **A614**, 415 (1997); E.L. Bratkovskaya, W. Cassing, and U. Mosel, *ibid.* **A622**, 593 (1997).

[36] A. Sibirtsev and W. Cassing, Nucl. Phys. **A641**, 476 (1998).

[37] G.Q. Li and G. Brown, Phys. Rev. C **58**, 1698 (1998).

[38] W. Cassing and E. Bratkovskaya, Phys. Rep. **308**, 65 (1999).

[39] D. Miśkowiec *et al.*, Phys. Rev. Lett. **72**, 3650 (1994).

[40] W. Ahner *et al.*, Phys. Lett. B **31**, 393 (1997).

[41] Y. Shin *et al.*, Phys. Rev. Lett. **81**, 1576 (1998).

[42] R. Barth *et al.*, Phys. Rev. Lett. **78**, 4007 (1997).

[43] F. Laue *et al.*, Phys. Rev. Lett. **82**, 1640 (1999).

[44] M. Menzel *et al.*, Phys. Lett. B **495**, 26 (2000); Ph.D. thesis, Universität Marburg, 2000.

[45] C. Sturm *et al.*, Phys. Rev. Lett. **86**, 39 (2001).

[46] J. Ritman *et al.*, Z. Phys. A **352**, 355 (1995).

[47] D. Best *et al.*, Nucl. Phys. **A625**, 307 (1997).

[48] P. Crochet *et al.*, Phys. Lett. B **486**, 6 (2000).

[49] A. Förster, Ph.D. thesis, Tu Darmsadt, 2002.

[50] L. Ahle *et al.*, E802 Collaboration, Phys. Rev. C **58**, 3523 (1998); **60**, 044904 (1999); E866/E917 Collaboration, Phys. Lett. B **476**, 1 (2000); **490**, 53 (2000).

[51] J. Harris, STAR Collaboration, Nucl. Phys. **A698**, 64 (2001).

[52] J.C. Dunlop and C.A. Ogilvie, Phys. Rev. C **61**, 031901 (2000), and references therein; C.A. Ogilvie, Nucl. Phys. **A698**, 39 (2001); J. C. Dunlop, Ph.D. thesis, MIT, 1999.

[53] Ch. Hartnack, H. Oeschler, and J. Aichelin, Phys. Rev. Lett. **90**, 102302 (2003).

[54] P. Koch, B. Müller, and J. Rafelski, Phys. Rep. **142**, 167 (1986).

[55] E.L. Bratkovskaya, W. Cassing, C. Greiner, M. Effenberger, U. Mosel, and A. Sibirtsev, Nucl. Phys. **A675**, 661 (2000).

[56] J. Cleymans and K. Redlich, Phys. Rev. Lett. **81**, 5284 (1998).

[57] J. Cleymans and H. Oeschler, J. Phys. G **25**, 281 (1999).

[58] J. Cleymans, D. Elliot, A. Keränen, and E. Suhonen, Phys. Rev. C **57**, 3319 (1998).

[59] J. Cleymans, H. Oeschler, and K. Redlich, Phys. Rev. C **59**, 1663 (1999).

[60] J. Cleymans and K. Redlich, Phys. Rev. C **60**, 054908 (1999).

[61] J. Cleymans, H. Oeschler, and K. Redlich, Phys. Lett. B **485**, 27 (2000).

[62] G.E. Brown, M. Rho, and C. Song, Nucl. Phys. **A690**, 184c (2001); **A698**, 483c (2002).

[63] R. Hagedorn and K. Redlich, Z. Phys. C **27**, 541 (1985).

[64] S. Balberg and A. Gal, Nucl. Phys. **A625**, 435 (1997).

[65] J. Mares, E. Friedman, A. Gal, and B.K. Jennings, Nucl. Phys. **A594**, 311 (1995).

[66] J. Dabrowski, Phys. Rev. C **60**, 025205 (1999).

[67] S. Bart *et al.*, Phys. Rev. Lett. **83**, 5238 (1999).

[68] E. Oset and A. Ramos, Nucl. Phys. **A679**, 616 (2001).

[69] M. Nekipelov *et al.*, Phys. Lett. B **540**, 207 (2002).

[70] L. Tolós, A. Polls, and A. Ramos, in *Proceedings of Mesons and Light Nuclei, Prague, Czech Republic*, edited by J. Adam, P. Bydzovsky, and J. Mares (AIP Conference Proceedings, Melville, NY, 2001), Vol. 603.

[71] R. Machleidt, Adv. Nucl. Phys. **19**, 189 (1989).

[72] A. Forster *et al.*, J. Phys. G **28**, 2011 (2002).

[73] S.A. Bass *et al.*, Prog. Part. Nucl. Phys. **41**, 225 (1998).

[74] E.L. Bratkovskaya, W. Cassing, and U. Mosel, Phys. Lett. B **424**, 244 (1998).

[75] E.L. Bratkovskaya, W. Cassing, R. Rapp, and J. Wambach, Nucl. Phys. **A634**, 168 (1998).

[76] W. Cassing, L. Tolós, E.L. Bratkovskaya, and A. Ramos, nucl-th/0304006.